Chapter 2

The redshifted H I 21-cm signal: a cosmological probe

Hyperfine coupling of the proton and electron spins in the ground state of the Hydrogen atom creates a triplet and a singlet state with the triplet state having a higher energy than the singlet state. A resonant transition between these spin-flip states results in the emission/absorption of radiation with wavelength of 21-cm (frequency 1420MHz) in the rest frame of the gas. Observation of this 21-cm radiation is hence a direct probe of the cosmological neutral hydrogen.

The radiative transfer equation describes the propagation of the radiation through the IGM.

$$\frac{dI_\nu}{ds} = -\alpha_\nu I_\nu + j_\nu \tag{2.1}$$

where I_ν is the intensity of the incident light and α_ν is the absorption coefficient. This equation may be expressed in terms of optical depth ($d\tau_\nu = \alpha_\nu ds$) and source function ($S_\nu = \frac{j_\nu}{\alpha_\nu}$) as

$$\frac{dI_\nu}{d\tau_\nu} = -I_\nu + S_\nu \tag{2.2}$$

The source function in thermal equilibrium is given by

$$S_\nu = \frac{2h\nu^3/c^2}{exp^{\frac{h\nu}{K_B T}} - 1} \tag{2.3}$$

In the case when the source function does not include the intensity I_ν the solution of this equation is given by

$$I_\nu = I_\nu(0)exp(-\tau_\nu) + S_\nu[1 - exp(-\tau_\nu)] \tag{2.4}$$

In a state of equilibrium the ratio of occupancy of the hyperfine levels is controlled by the of the spin temperature T_s defined by

$$\frac{n_1}{n_0} = 3 \exp\left\{-\frac{\mathrm{T_*}}{\mathrm{T_s}}\right\}, \tag{2.5}$$

where n_0 and n_1 denote the populations in the triplet and the singlet states respectively. Here $T_* = h_p\nu_e/k_B = 0.068K$, where h_p is the Plank's constant, $\nu_e = 1420$MHz and k_B denotes the Boltzmann's constant. Along a line of sight $\mathbf{n}$, the CMBR photons interact with the intervening H I through the 21-cm transition. According to the radiative transfer equation and relating the intensity to temperature as $I = 2k_BT/\lambda^2$ we have the change in the CMBR brightness temperature ([26]) given by

$$T(\tau) = T_\gamma e^{-\tau} + T_s(1 - e^{-\tau}) \tag{2.6}$$

where τ is the 21-cm optical depth, and T_γ is the temperature of the background CMBR.

The quantity of observational interest for radio observations of the 21-cm radiation is the excess brightness temperature redshifted to the observer at present defined as

$$T_b(\mathbf{n}, z) = \frac{T(\tau) - T_\gamma}{1+z} \approx \frac{(T_s - T_\gamma)\tau}{1+z} \tag{2.7}$$

where we have assumed that $\tau << 1$ and CMBR anisotropies are neglected. The 21-cm optical depth at a redshift z and along a line of sight $\mathbf{n}$ and is given by ([27])

$$\tau = \frac{4.0\mathrm{mK}}{T_s}\left(\frac{\Omega_b h^2}{0.022}\right)\left(\frac{0.7}{h}\right)\frac{H_0}{H(z)}(1+z)^3\frac{\rho_{\mathrm{HI}}}{\bar{\rho}_{\mathrm{H}}}\left[1 - \frac{(1+z)}{H(z)}\frac{\partial v}{\partial r_\nu}\right] \tag{2.8}$$

where the comoving distance r_ν is given by

$$r_\nu = \int_0^z dz' \frac{c}{H(z')}. \tag{2.9}$$

H(z) is the Hubble parameter which is sensitive to the cosmological model, v denotes the peculiar velocity component along the sight line and $\frac{\rho_{\mathrm{HI}}}{\bar{\rho}_{\mathrm{H}}}$ is the ratio of the neutral hydrogen to the mean hydrogen density. We may write as in ([27])

$$\delta T_b(\nu, \hat{\mathbf{n}}) = \bar{T}(z)\ \eta_{\mathrm{HI}}\left(z, \hat{\mathbf{n}} r_\nu\right) \tag{2.10}$$

where the redshift dependent quantity $\bar{T}(z)$ is given by

$$\bar{T}(z) = 4\mathrm{mK}(1+\mathrm{z})^2 \left(\frac{\Omega_\mathrm{b}\mathrm{h}^2}{0.022}\right)\left(\frac{0.7}{\mathrm{h}}\right)\frac{\mathrm{H}_0}{\mathrm{H(z)}} \tag{2.11}$$

and

$$\eta_{\mathrm{HI}}(z,\hat{\mathbf{n}}r_\nu) = \bar{x}_{\mathrm{HI}}(z)\left\{\left(1-\frac{T_\gamma}{T_s}\right)\left[\delta_H(\hat{\mathbf{n}},z) - \frac{(1+z)}{H(z)}\frac{\partial v(z,\hat{\mathbf{n}}r_\nu)}{\partial r_\nu}\right] + \frac{T_\gamma}{T_s}s\ \delta_H(\hat{\mathbf{n}},z)\right\} \tag{2.12}$$

The quantity $\bar{x}_{\mathrm{HI}}(z)$ denotes the mean neutral fraction at a redshift z, and $\delta_H(\hat{\mathbf{n}},z)$ is the H I perturbations. The function s relates the fluctuations of the spin temperature to the H I fluctuations. The H I fluctuations are modelled to be related to the underlying dark matter fluctuations through a possible bias $b(k)$. Thus $\delta_H(\hat{\mathbf{n}},z) = b(k)\ \delta(\hat{\mathbf{n}},z)$ where δ denotes the dark matter fluctuations. We define the power spectrum P_{HI} as

$$\bar{T}(z)^2\langle\tilde{\eta}_{\mathrm{HI}}(\mathbf{k},z)\tilde{\eta}_{\mathrm{HI}}(\mathbf{k}',z)\rangle = (2\pi)^3\delta_D^3(\mathbf{k}-\mathbf{k}')P_{\mathrm{HI}}(\mathbf{k},z)\,. \tag{2.13}$$

where $\tilde{\eta}_{\mathrm{HI}}(\mathbf{k},z)$ is the Fourier transform of $\eta_{\mathrm{HI}}(z,\hat{\mathbf{n}}r_\nu)$ given by

$$\eta_{\mathrm{HI}}(z,\hat{\mathbf{n}}r_\nu) = \int\frac{d^3\mathbf{k}}{(2\pi)^3}\mathrm{e}^{-\mathrm{i}kr_\nu(\hat{\mathbf{k}}\cdot\hat{\mathbf{n}})}\tilde{\eta}_{\mathrm{HI}}\,(z,\mathbf{k}) \tag{2.14}$$

and

$$f = \frac{dlnD_+}{dlna} \tag{2.15}$$

is the rate of growth of perturbations with D_+ denoting the growing mode of density fluctuations. Thus we have

$$P_{\mathrm{HI}}(\mathbf{k},z) = \bar{T}(z)^2\bar{x}_{\mathrm{HI}}(z)^2\left[\left(1-\frac{T_\gamma}{T_s}\right)\left(\ b(k)+f(\hat{\mathbf{k}}\cdot\hat{\mathbf{n}})^2\right)+\frac{T_\gamma}{T_s}s\ \right]^2 P(k,z) \tag{2.16}$$

where $P(k,z)$ is the dark matter power spectrum.

2.0.1 Evolution of the Spin temperature

Around a redshift $z\sim 1000$ primordial plasma has cooled sufficiently to allow protons and electrons to combine and form neutral hydrogen and the Universe enters into Dark ages. This era continues till the formation of the first luminous

objects at $z \sim 30$. Although most of the electrons and protons combine together to form the bound state, a small fraction of electron will survive in this process of recombination. Collisional processes involving a tiny fraction of electrons which survived recombination at $z \sim 1000$ tries to keep the kinetic temperature of the gas T_g at the same value as the CMBR temperature. These collisional couplings becomes ineffective at $z \sim 200$. Thus, in the absence of external heating $T_g \propto (1+z)^2$ while $T_\gamma \propto (1+z)$. The spin temperature T_s continues to be coupled to T_g till $z \sim 70$ through collisional spin flipping after which it approaches T_γ again.

At lower redshifts and after the formation of luminous sources, the population of the hyperfine triplet state increases due to Lyman-α scattering, through the Wouthuysen-Field effect ([28]). and thus $T_s >> T_\gamma$ at low redshifts.

The 21-cm radiation will only be seen when $T_s \neq T_\gamma$. Therefore, in the redshift window $30 \leq z \leq 200$ where $T_s < T_\gamma$ H I is expected to be seen in absorption against the background CMBR. At lower redshifts when $T_s > T_\gamma$, the redshifted 21-cm radiation would be seen in emission. The evolution of T_s and T_g are discussed in details in [27, 29].

The 21-cm line allows radio observations to tomographically image the entire 3D volume in the redshift range $0 \leq z \leq 200$ by tuning the observing frequency of radio telescope. The entire volume is divided into three regions.

1. The dark ages - this corresponds to the epoch $20 < z < 200$. and ends with the epoch when the first luminous sources are formed.

2. The epoch of Reionization - this corresponds to the epoch approximately $6 < z < 20$. starting with the formation of first star and ending with the phase transition of the Universe from neutral to ionized state.

3. The post-reionization epoch - this is the era from the end of the reionization process upto the present $z = 0$.

The neutral fraction evolves from its value $x_{H\ i} \sim 1$ in the "dark ages" to its present value $\sim 10^{-3}$ and traces the astrophysical processes characterizing these epochs.

2.0.2 The Dark Ages

The era between the epoch of recombination $z \sim 1000$ when neutral hydrogen formed and the formation of first stars is known as the "dark age". CMBR photons already decoupled from matter, and thus do not contain any direct cosmological imprint from this epoch. Since the neutral fraction is close to unity, the 21-cm radiation from neutral hydrogen has the possibility of probing the cosmological

evolution and structure formation in this epoch. The 21-cm signal is "seen" only if the spin temperature differs from the CMBR temperature. In the dark ages corresponding to $20 \leq z \leq 200$ we know that $T_s < T_\gamma$ and thus the hyperfine spin flip process resonantly absorbs the CMB photons. The 21-cm signal thus manifest as an absorption feature in CMBR spectrum ([29]).

Matter density fluctuations in the dark ages is in the linear regime and the evolution of perturbations can be adequately analyzed using linear perturbation theory. Fluctuations in the HI can also be assumed to faithfully trace the underlying dark matter fluctuations allowing for an easy analytical study of the statistical properties of the signal. Thus the HI signal from the pre-reionization epoch is largely determined by the dark matter power spectrum. There has been extensive theoretical investigations to study the "dark ages" through the 21-cm observations ([8, 30–39]). The measurement of the HI power spectrum from the dark ages is known to be a potentially powerful probe of fundamental physics. Gravitational collapse leading to formation of the first stars at redshift $z \sim 20$ ([40–45]) brings about an end to this epoch. In dark ages all the hydrogen in the Universe is neutral, and the fluctuations in the HI density Δ_{HI} trace the dark matter fluctuations $\Delta_{HI}(\mathbf{k}, z) = \bar{\rho}_H \Delta(\mathbf{k}, z)$. Fluctuations of Δ_{HI} is related to fluctuations in the spin temperature ΔT_S given by $\Delta T_S = s(z) T_S \Delta_{HI}/\rho_{HI}$ where $s(z)$ is a dimensionless function. The Fourier transform of the "21 cm radiation efficiency in redshift space" becomes

$$\eta(\mathbf{k}, z) = \left[\left(1 - \frac{T_\gamma}{T_S}\right)\left(1 + f\mu^2\right) + \frac{T_\gamma}{T_S} s\right] \Delta(\mathbf{k}, z) \tag{2.17}$$

where μ is the cosine of the angle between $\mathbf{k}$ and the line of sight $n\widehat{n}$, and $f(\Omega_m) \approx \Omega_m^{0.6} + \frac{1}{70}\left[1 - \frac{1}{2}\Omega_m(1 + \Omega_m)\right]$ in a spatially flat universe [46]. The power spectrum of the 21-cm efficiency in terms of the dark matter power spectrum in the dark ages is given by

$$P_{HI}(k, z) = \left[\left(1 - \frac{T_\gamma}{T_S}\right)\left(1 + f\mu^2\right) + \frac{T_\gamma}{T_S} s\right]^2 P(k, z). \tag{2.18}$$

2.0.3 Epoch of Reionization

The formation of the first stars initiated the epoch of reionization. This epoch is of great importance in cosmology whereby the state of the universe changed from being completely neutral to being almost ionized by the radiation from the luminous sources. Owing to the complex astrophysical processes involved, our understanding

of this epoch remains greatly uncertain with many unanswered questions. Some of the important questions are about the precise time of "reionization", the actual nature of the astrophysical processes involved, the large scale H I distribution the relative contributions of different ionizing sources towards reionization, and the nature of various feedback processes. The beginning of the reionization process initiated various feedback mechanisms which had important effect on structure formation and cosmological evolution of the intergalactic medium ([45, 47, 48]).

Observation of Lyman -α forest indicating the absence of Gunn-Peterson troughs ([49]) in the absorption spectra of distant quasars indicate that the reionization was complete at around $z \sim 6$ ([50–52]). WMAP measurements of the electron scattering optical depth τ_e from the CMBR temperature-polarization and polarization-polarization power spectra ([53–55]) point to the fact that reionization started before $z \sim 10$. It is now believed that the EoR extend over a redshift range $6 - 15$ ([56, 57]).

Unlike the CMBR observations which can measure the integrated effect of reionization, 21-cm EoR signal can be used for a tomographic study of the universe by suitably tuning the frequency of radio observation allowing for the study of EoR continuously over a wide range of redshifts. Several heating processes ([26, 58]) causes the spin temperature T_s to be much above the CMB temperature whereby the 21-cm radiation from the EoR is seen in emission.

The effect of the H I heating and its ionization on the 21-cm signal has been studied in great detail ([59–65]). Observationally, one is motivated to look at either the average 21-cm signal over large areas of the sky (global evolution of the neutral fraction) ([60]) or large scale statistical distribution of H I through quantities like the Power spectrum, Bispectrum from the EoR ([27, 66–68]). There is also the aim towards the detection of individual ionized bubbles as a direct probe of reionization and also quantify the properties of the ionizing sources([32, 69–71]).

The spin temperature depends on three processes:

1. Absorption or stimulated emission of CMB photons near the 21 cm transition leads to coupling between T_s and T_γ.

2. Collisional excitation and de-exications due to collisions between hydrogen atoms with other particles. This mainly includes collision between hydrogen atom with other hydrogen atoms, electrons and protons. The collision dominates in the dark ages where the density of hydrogen gas is high.

3. Spin flip via Wouthuysen-Field effect which arises due to Resonant scattering

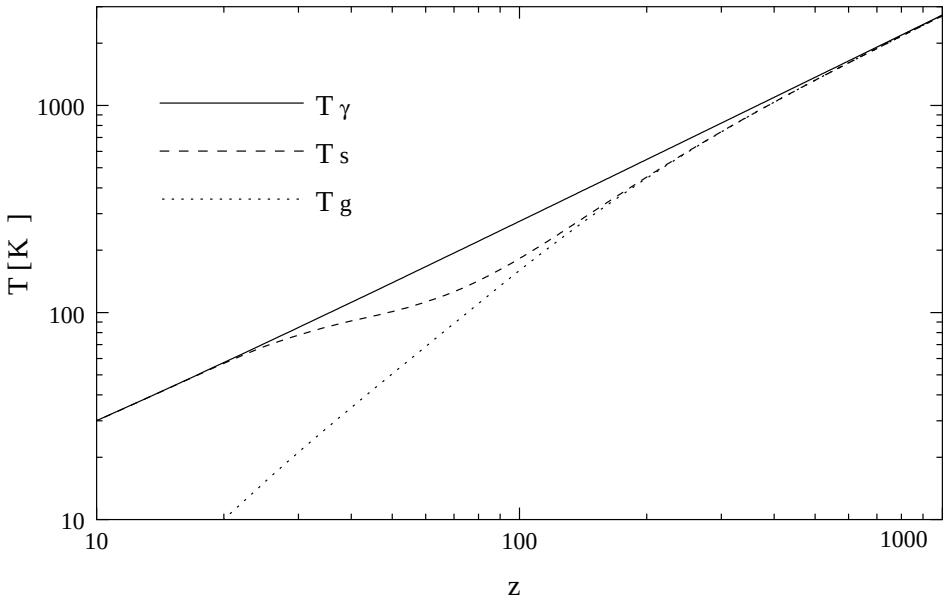

Figure 2.1: Evolution of Spin temperature

of Lyman-α photons from the stars. Wouthuysen-Field effect. If the atom is initially $1_1S_{1/2}$ state it will excite to $2_1P_{3/2}$, $2_2P_{1/2}$ hyperfine levels by absorption of a Ly-α photon. The other two hyperfine states are inaccessible due to selection rules. The exited atom can return to the either of the ground state by emitting a Ly-α photon and this can lead to a spin flip.

Variation of spin temperature can be approximated as

$$T_S^{-1} = \frac{T_\gamma^{-1} + x_\alpha T_\alpha^{-1} + x_c T_K^{-1}}{1 + x_\alpha + x_c}, \tag{2.19}$$

The HI gas is heated well before it is reionized, and that the spin temperature is coupled to the gas temperature so that $(1 - T_\gamma/T_S) \to 1$. Therefore, $\eta > 0$. Hence HI will be seen in emission. This emission depends only on the HI density and peculiar velocity. In this era a fraction of the volume f_V is ionized. The fraction of volume ionized f_V, and the mean neutral fraction $\bar{x}_{HI}$ and mean comoving number density of ionized spheres $\bar{n}_{HI}$ are related as $f_V = 1 - \bar{x}_{HI} = (4\pi R^3/3)\bar{n}_{HI}$. The mean neutral fraction is given by Zaldarriaga et al. (2003).

$$\bar{x}_{HI}(z) = \frac{1}{1 + \exp((z - z_0)/\Delta z)} \tag{2.20}$$

with $z_0 = 10$ and $\Delta z = 0.5$ therefore 50% of the hydrogen is reionized at a

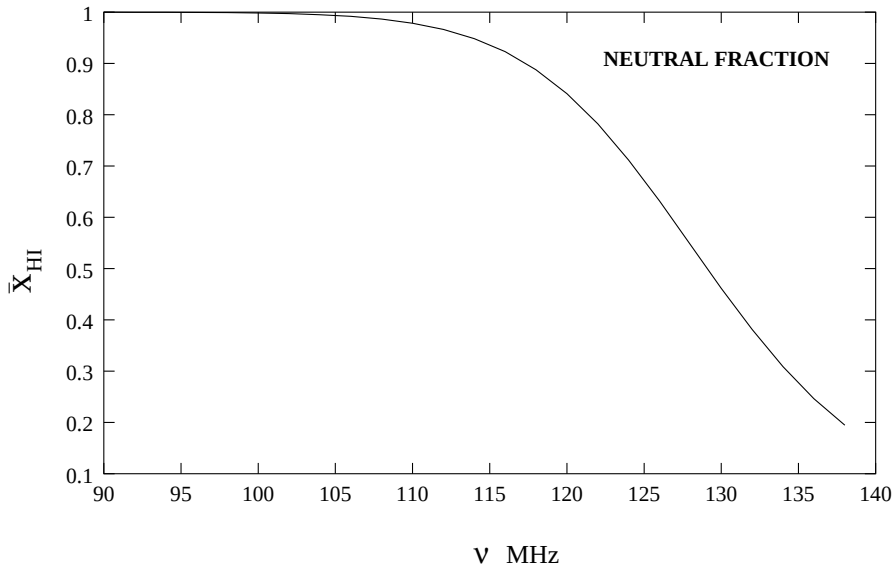

Figure 2.2: Evolution of the neutral fraction

redshift $z = 10$ (Figure 2.2). The non-overlapping spheres of comoving radius R are completely ionized, the centres of the spheres being clustered with a bias $b_c \geq 1$ relative to underlying dark matter distribution.

HI density is given by

$$\rho_{HI}(x,z) = \bar{\rho}_H(1+\delta)\left[1 - \sum_a \theta(\frac{\mathbf{x}-\mathbf{x_a}}{R})\right] \tag{2.21}$$

where δ is the dark matter fluctuation, a refers to the different ionized spheres with centers at x_a, and $\theta(y)$ is the Heaviside step function defined such that $\theta(y) = 1$ for $0 \leq y \leq 1$ and zero otherwise. We then have

$$\eta(x,z) = \left[1 + \delta - \frac{1+z}{H(z)}\frac{\partial v}{\partial r}\right]\left[1 - \sum_a \theta\left(\frac{\mathbf{x}-\mathbf{x_a}}{R}\right)\right]. \tag{2.22}$$

The Fourier transform of the first term in the square bracket of eq. (2.22) is

$$(2\pi)^3\delta_D^3(\mathbf{k}) + (1+\mu^2)\Delta(k,z), \tag{2.23}$$

and the Fourier transform of the second term is

$$(2\pi)^3\delta_D^3(\mathbf{k}) - (4\pi R^3/3)W(kR)\sum_a e^{ik\cdot x_a} \tag{2.24}$$

where, $W(y) = (3/y^3)[sin(y) - ycos(y)]$ is the spherical top hat window function. The term $\sum_a e^{i\mathbf{k}\cdot x_a}$ is the Fourier transform of the distribution of the centers of the ionized spheres which we write as $\sum_a e^{i\mathbf{k}\cdot x_a} = \bar{n}_{HI}[(2\pi)^3\delta^3_{D(k)} + \Delta_{P(k,z)} + b_c\Delta(k,z)]$, where $\Delta_{P(k,z)}$ is the fluctuation in the distribution of the centers arising due to the discrete nature of these points (Poisson fluctuations) and the term $b_c\Delta(k,z)$ arises due to the clustering of the centers. These two components of the fluctuation are independent and $\langle\Delta_P(\mathbf{k})\Delta_P^*(\mathbf{k}')\rangle = (2\pi)^3\delta_D^3(\mathbf{k}-\mathbf{k}') \times 1/\bar{n}_{HI}$. Convolving the Fourier transform of the two terms in eq. (2.22), and dropping terms of order Δ^2 and $\Delta\Delta_P$ we have

$$\begin{aligned}\eta(k,z) &= \left[\bar{x}_{HI}(1+f\mu^2) - b_c f_V W(kR)\right]\Delta(k,z) \\ &- f_V W(kR)\Delta_P(k,z)\end{aligned} \tag{2.25}$$

This gives the power spectrum of the " 21 cm emission efficiency in redshift space"

$$\begin{aligned}P_{HI}(k,z) &= \left[\bar{x}_{HI}(1+f\mu^2) - b_c f_V W(kR)\right]^2 P(k,z) + \\ &+ \frac{f_V^2 W^2(kR)}{\bar{n}_{HI}}\end{aligned} \tag{2.26}$$

The first term which contains $P(k)$ arises from the clustering of the hydrogen and the clustering of the centers of the ionized spheres. The second Poisson term which has $1/\bar{n}_{HI}$ arises due to the discrete nature of the ionized regions.

2.1 The post-reionization era

The post-reionization IGM is predominantly ionized. While the low density gas gets completely ionized by the end of reionization, a small fraction of neutral hydrogen survives and most of the neutral gas remains confined to the over-dense regions of the IGM which are self shielded from ionizing radiation. The H I signal from the post-reionization epoch has been extensively studied [72–79].

In the post-reionization epoch, two astrophysical systems are of great observational relevance

- the low density, optically thin Lyman-α absorbers. They produce distinct

absorption feature in the spectra of background quasars called the Lyman-α forest.

- the clumped, dense damped Lyman-α systems (DLAs) [80] which are self shielded from background ionizing radiation. These DLAs store $\sim 80\%$ of the H I at $z < 4$ [81] with H I column density greater than 2×10^{20}atoms/cm^2 [82–84]. The distribution and clustering properties of the DLA clouds suggest that they are associated with galaxies which are located in regions of highly non-linear matter over densities [85–87]. These clouds are the dominant source of the 21-cm radiation in the post reionization epoch.

The densely clumped H I regions though source the 21-cm emission, do not contribute to the Lyman-α optical depth. However the 21-cm flux from individual clouds is extremely weak ($< 10\mu$Jy). These individual clouds are unlikely to be detected in radio observations, even with futuristic telescopes though there may be some enhancement of the signal due to the effect of gravitational lensing by intervening matter [88].

In this epoch the population of the triplet state of H I is increased greatly due to Wouthuysen field coupling. This makes the spin temperature T_s much greater than the CMB temperature T_γ, whereby $(T_s - T_\gamma)/T_s \sim 1$ and since $T_s >> T_\gamma$ the 21-cm radiation is seen in emission in this epoch against the background CMBR [26, 27, 29].

Extensive study of the Lyman-α absorption lines in quasar spectra indicates that in the redshift range $1 \leq z \leq 3.5$ the cosmological density parameter of the neutral gas has a value $\Omega_{gas} \sim 10^{-3}$ [81]. This is equivalent to saying that the mean neutral fraction $\bar{x}_{\rm HI} = \Omega_{gas}/\Omega_b \sim 2.45 \times 10^{-2}$. The mean neutral fraction does not evolve in the post-reionization epoch. A non-zero neutral fraction implies there would be a 21-cm signal even after the completion of reionization at $z \sim 6$.

2.1.1 Modeling the post-reionization H I

Several simplifying assumptions are used in the modelling of the post-reionization H I signal. These are either motivated from implicit observations or from numerical simulations.

1. The spin-temperature rises well above the CMBR temperature ie $T_s >> T_\gamma$. For $z \leq 6$ the spin temperature and the gas kinetic temperature are strongly coupled through Lyman-α scattering or collisional coupling [26].

2. The mean neutral hydrogen fraction $\bar{x}_{\rm HI}$ is a constant in the entire redshift range $z \leq 6$.

3. On the large scale the H I peculiar velocities are assumed to be determined by dark matter fluctuations. The effect of the peculiar velocity is the redshift space distortion which produces an anisotropy in the signal.

4. The H I is assumed to trace the dark matter distribution with a possible bias $b_T(k, z)$. The background ionizing background on the neutral fraction may also contribute to $b_T(k, z)$. The bias is scale dependent on small scales comparable to the Jean's scale. On large scales a linear constant bias is consistent with simulations.

5. Though the 21-cm signal is sourced by DLA clouds, the discrete nature of these emitters is not considered. The corresponding Poisson noise owing to this discrete sampling is neglected assuming that the number density of the DLA emitters is very large [78].

6. The gas distribution follows the underlying dark matter distribution whose fluctuations are primordially generated by a Gaussian random process. We do not consider any non-gaussianity and thereby the statistical information is contained in the two-point correlation or the power spectrum.

2.1.2 Post-reionization H I bias

Galaxy redshift surveys and numerical simulations reveal that the galaxies trace the underlying dark matter distribution with a bias [89–91]. Assuming that the H I in the post-reionization epoch are mostly housed in dark matter haloes we may assume that the gas traces the underlying dark matter distribution with a bias $b_T(k, z)$ defined as

$$b_T(k, z) = \left[\frac{P^{\rm HI}(k, z)}{P(k, z)}\right]^{1/2} \tag{2.27}$$

where $P^{\rm HI}(k, z)$ and $P(k, z)$ denote the H I and dark matter power spectra respectively. The bias quantifies the nature of H I clustering in the post-reionization epoch.

On scales below the Jean's length, the linear density contrast of H I gas is related to the dark matter density contrast though a scale dependent function [92]. However the bias is known to be scale-independent on large scales, though the scales above which the bias is linear, is sensitive to the redshift being probed.

Numerical simulations show that the large scale linear bias grows monotonically with redshift for $1 < z < 4$ [93]. This feature is shared by galaxy bias as well [90, 94, 95]. Several authors have now demonstrated the nature of H I bias using N-body simulations [96–100]. A fitting formula for the bias $b_T(k, z)$ as a function of both redshift and scale has been obtained from numerical simulations [98, 99]. We have used these simulation results in our modelling of the post-reionization epoch. It can be noted that a linear bias model is a reasonably good approximation on large scale. However the product $b_T^2(k, z)\bar{x}_{\rm HI}$ which appears in the overall amplitude of the 21-cm signal is a largely unknown parameter.

2.1.3 Power spectrum of H I fluctuations from the post-reionization epoch

The H I 21-cm brightness temperature fluctuations from redshift $z_{\rm HI}$ in Fourier space is related to the underlying dark matter overdensity field $\delta(\mathbf{k}, z)$ as [27]

$$\Delta_{\rm HI}(\mathbf{k}) = \bar{T}\bar{x}_{\rm HI}(b_T + f\mu^2)\delta(\mathbf{k}, z) \tag{2.28}$$

where $\bar{x}_{\rm HI}$ is the mean H I fraction, $\mu = \hat{\mathbf{k}} \cdot \hat{\mathbf{n}}$ and

$$\bar{T}(z) = 4.0\,{\rm mK}\,(1+z)^2 \left(\frac{\Omega_{b0}h^2}{0.02}\right)\left(\frac{0.7}{h}\right)\frac{H_0}{H(z)} \tag{2.29}$$

The term $f\mu^2$ has its origin in the H I peculiar velocities [27, 76] which, as we mentioned is also sourced by the dark matter fluctuations.

Note that one should, in principle include a normalized window function $\mathcal{W}(z)$ in eq.(2.28) describing the spectral response of an instrument [101]. On scales of our interest ($k \lesssim 100/r$), the spectral resolution of the instrument can however be assumed to be much smaller than the features in the H I signal [66, 75] and $\mathcal{W}(z)$ can be approximated by a Dirac delta function, so that eq. (2.28) is, a reasonably good approximation. Thus the 21-cm H I power spectrum from the post reionization era given by [102]

$$P_{\rm HI}(\mathbf{k}, z) = \bar{T}(z)^2\bar{x}_{\rm HI}^2(b_T + f\mu^2)^2 P(k, z) \tag{2.30}$$

where all the terms have been defined earlier.

2.1.4 Cosmology with 21-cm observations from the post-reionization era

The redshifted 21-cm signal from the post-reionization epoch [75, 76, 103–106] as a biased tracer of the dark matter distribution has the potential to probe the cosmological background evolution and structure formation. Observationally the post-reionization signal has two advantages - Firstly since the Galactic synchrotron foreground scales as $\sim (1+z)^{2.6}$, the lower redshifts are least affected by the galactic foreground. Secondly, in the redshift range $z \leq 6$ the complex astrophysical processes of the EoR are absent. Thus the background UV radiation field does not have any feature imprinted on the 21-cm signal.

The 21-cm emission from individual DLA clouds in the post reionization era, is too weak to be resolved in observations. However the collective signal forms a diffused background in all radio-observations at the observation frequencies less than 1420 MHz. The fluctuations in this background emission on the sky plane (angular variations) and across redshift (frequency), maps out the three dimensional tomographic image of the Universe. The statistical properties of the fluctuations are quantified though the power spectrum discussed in the last section imprints the background evolution of the Universe, growth of perturbations, and astrophysics of the diffuse IGM. The intensity mapping of the 3D power spectrum of the 21-cm signal has the potential for precision cosmology over a wide range of redshifts and scales.

The intensity mapping [107] of the post-reionization 21-cm signal has been proposed as a tool for cosmological parameter estimation [102, 104–106, 108–110] using futuristic radio telescopes. The anisotropy in the redshift space has been suggested as a method to separate the astrophysical component from the cosmology [103]. Such observations maybe used to determine the redshift space distortion parameter and other observables relevant to the background cosmology [102]. Baryon acoustic oscillation (BAO) is a powerful tool used to constant dark energy models. The measurement of the BAO distance scale through its oscillatory signature in the post-reionization power spectrum has been proposed [111] (for $z > 3$) and [107] has investigated the redshift range ($z < 2$) for BAO features in the 21-cm observations as a probe of dark energy. Other than constraining cosmological models, the post-reionization 21-cm power spectrum may also be used to constrain galaxy bias for DLA host galaxies [112] and cosmological H I mass density [23].

Most of the literature concur that the next generation dedicated radio-interferometric observations of the post-reionization epoch will yield competitive if not signif-

icantly better constraints on cosmology than the next generation supernova Ia observations, galaxy surveys, and CMB experiments.

2.2 Observational challenges

Over the last decade there has been a massive global quest towards detecting the cosmological H I through radio-observations of the redshifted 21-cm line. These initiatives are driven by the promise of rich cosmological information that such observations have the potential to provide [113, 114].

Some of these attempts aim towards detecting the global H I signal using small single dish with large field of view (experiments like the CORE and EDGES[1] fall in this category) Most of the ongoing and upcoming 21-cm missions, however aim towards H I intensity mapping.

The 21-cm intensity mapping involves large volume and low resolution statistical measurement of the cosmological H I fluctuations as a function of scale, through radio-interferometric observations. Several radio telescopes, like the currently functioning Giant Metre-Wave Radio Telescope (GMRT[2]) and upcoming instruments like (e.g., MWA[3], LOFAR[4], 21 CMA [5], PAPER[6], VLA extension program[7] OWFA [8] and SKA[9]), aim towards a 3D mapping of the 21-cm sky. Low resolution compact interferometers with wide fields-of-view covering large survey volumes are now understood to be best suited for precision cosmology at the BAO scale [107, 111]. The focus is on the large scale fluctuations from H I in DLAs without an attempt to resolve them. These 21-cm intensity mapping experiments include CHIME (Canadian Hydrogen Intensity Mapping Experiment) and the related CRT (Cylinder Radio Telescope) telescopes.

Detecting the cosmological 21-cm signal is extremely challenging. The signal is sunk deep under foregrounds which are ~ 5 orders-of-magnitude larger [14, 64]. The foregrounds primarily arise from astrophysical sources like Synchrotron radiation from our own galaxy, free free emission, or extra-galactic radio point sources [13, 15, 60, 115]. The cosmological signal is also plagued by terrestrial RFI (ra-

[1] http://haystack@mit.edu
[2] http://www.gmrt.ncra.tifr.res.in
[3] http://www.haystack.mit.edu/ast/arrays/mwa/
[4] http://www.lofar.org/
[5] http://web.phys.cmu.edu/~past/
[6] http://astro.berkeley.edu/~dbacker/eor/
[7] http://www.cfa.harvard.edu/dawn/
[8] http://www.ncra.tifr.res.in/ncra/ort
[9] http://www.skatelescope.org/

dio frequency interferences) from mobile phones, satellite broadcasts and other instrumental effects. Detectability of the H I signal at a high level of statistical significance rests on mitigating these effects and precise removal of the contaminants [116].

There is extensive research dealing with foreground removal using theoretical methods and numerical simulations.

A promising proposal uses the spectral property of the the multi frequency angular power spectrum (MAPS)[68]. In this method one correlates the H I from two redshift slices. While the H I signal is expected to decorrelate quickly over a frequency separation $\Delta\nu \sim 1$MHz, the foregrounds having a continuous spectra are expected to remain correlated. By removing the smooth component the signal may be separated. Another suggested technique for foreground removal is to subtract any smooth frequency dependent component either from the image cube [117–121] or from the gridded visibilities [16]. The multi-frequency analysis to separate out the foregrounds has been studied in [14, 66, 68].

Though sensitive removal of large foregrounds is the key problem, several other crucial issues like instrumental noise, calibration errors and tackling the man made radio frequency interferences (RFI) also pose challenges towards the detection of the H I signal.

In this thesis we focus on the proposal of cross-correlating the 21-cm signal with other tracers as a way to bypass the foreground issue to some reasonable extent.